Available online at www.sciencedirect.com
ScienceDirect
Geochimica et Cosmochimica Acta 73 (2009) 5584–5599
Geochimica et Cosmochimica Acta
www.elsevier.com/locate/gca

Influence of pH and dissolved Si on Fe isotope fractionation during dissimilatory microbial reduction of hematite

Lingling Wu *, Brian L. Beard, Eric E. Roden, Clark M. Johnson

Department of Geoscience, University of Wisconsin-Madison, 1215 West Dayton Street, Madison, WI 53706, United States
NASA Astrobiology Institute, University of Wisconsin-Madison, Madison, WI 53706, United States

Received 13 January 2009; accepted in revised form 30 June 2009; available online 7 July 2009

Abstract

Microbial dissimilatory iron reduction (DIR) has been identified as a mechanism for production of aqueous Fe(II) that has low $^{56}Fe/^{54}Fe$ ratios in modern and ancient suboxic environments that contain ferric oxides or hydroxides. These studies suggest that DIR could have played an important role in producing distinct Fe isotope compositions in Precambrian banded iron formations or other marine sedimentary rocks. However, the applicability of experimental studies of Fe isotope fractionation produced by DIR in geochemically simple systems to ancient marine environments remains unclear. Here we report Fe isotope fractionations produced during dissimilatory microbial reduction of hematite by *Geobacter sulfurreducens* in the presence and absence of dissolved Si at neutral and alkaline pH. Hematite reduction was significantly decreased by Si at alkaline (but not neutral) pH, presumably due to Si polymerization at the hematite surface. The presence of Si altered Fe isotope fractionation factors between aqueous Fe(II) or sorbed Fe(II) and reactive Fe(III), reflecting changes in bonding environment of the reactive Fe(III) component at the oxide surface. Despite these changes in isotopic fractionations, our results demonstrate that microbial Fe(III) oxide reduction produces Fe(II) with negative $\delta^{56}Fe$ values under conditions of variable pH and dissolved Si, similar to the large inventory of negative $\delta^{56}Fe$ in Neoarchean and Paleoproterozoic age marine sedimentary rocks.

1. INTRODUCTION

Bacterial dissimilatory iron reduction (DIR) is a major pathway of organic carbon oxidation in modern marine sediments where reactive Fe(III) hydroxides are present (e.g., Lovley, 1991; Thamdrup, 2000). A flux of organic carbon driven by anoxygenic CO_2 fixation coupled to Fe(II) oxidation (Cloud, 1965; Garrels et al., 1973; Widdel et al., 1993) could have supplied the organic carbon and Fe(III) required to facilitate DIR in the early Earth (Lovley, 2000). DIR has been hypothesized to have played an important role in producing distinct Fe isotope compositions in Precambrian banded iron formations (BIFs) or other marine sedimentary rocks (Staubwasser et al., 2004; Yamaguchi et al., 2005; Bergquist and Boyle, 2006; Severmann et al., 2006; Jenkyns et al., 2007; Johnson et al., 2008a,b; Severmann et al., 2008). Experimental studies of Fe isotope fractionation produced by DIR, however, have been limited to date in exploring the effects of pH and dissolved ions, potentially limiting the applicability of previous studies to conditions that were analogous to ancient marine environments.

A number of experimental studies have shown that aqueous Fe(II) produced by DIR has low $^{56}Fe/^{54}Fe$ ratios relative to the initial Fe(III) substrate (Beard et al., 1999, 2003; Crosby et al., 2005, 2007). Experimental studies by Crosby et al. (2005, 2007) provided an important breakthrough in identifying the fundamental mechanism for Fe isotope fractionation during DIR, which involves coupled electron transfer and atom (isotope) exchange between aqueous Fe(II) ($Fe(II)_{aq}$) and a reactive Fe(III) component ($Fe(III)_{reac}$) on the Fe(III) oxide surface (Fig. 1). Bacteria are envisioned to catalyze isotopic exchange between

* Corresponding author. Address: Department of Geology and Geophysics, University of Wisconsin-Madison, 1215 West Dayton Street, Madison, WI 53706, United States. Tel.: +1 608 890 0929.
E-mail address: lwu@geology.wisc.edu (L. Wu).

0016-7037/$ - see front matter © 2009 Elsevier Ltd. All rights reserved.
doi:10.1016/j.gca.2009.06.026

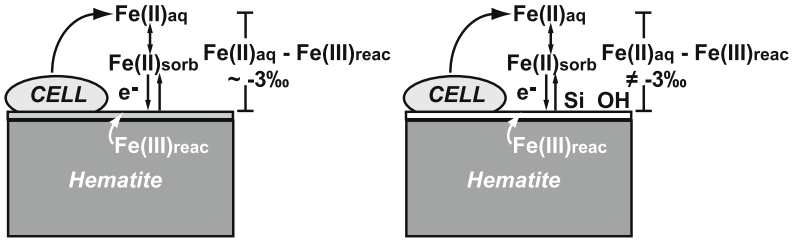

Fig. 1. Schematic illustration of bacterial reduction of hematite (modified after Crosby et al., 2007, not to scale). Part of the aqueous Fe(II) ($Fe(II)_{aq}$) produced sorbs to hematite surface ($Fe(II)_{sorb}$), and then undergoes electron transfer and Fe(II)–Fe(III) atom exchange, producing a reactive layer of Fe(III) at the oxide surface ($Fe(III)_{reac}$) that has $^{56}Fe/^{54}Fe$ ratios which are higher than those of the initial hematite, balanced by $Fe(II)_{aq}$ that has $^{56}Fe/^{54}Fe$ ratios which are lower than the initial hematite. The left side shows overall isotopic fractionation between $Fe(II)_{aq}$ and $Fe(III)_{reac}$ of $\sim -3‰$, the expected fractionation where $Fe(III)_{reac}$ is hematite. The right side, however illustrates the changes observed in this study in the presence of Si, and at high pH, where fractionation between $Fe(II)_{aq}$ and $Fe(III)_{reac}$ does not reflect that of the equilibrium $Fe(II)_{aq}$-hematite fractionation, suggesting $Fe(III)_{reac}$ is a phase other than hematite or that Fe bonding is significantly different than that in the Si-absent, circum-neutral pH experiments.

$Fe(II)_{aq}$ and $Fe(III)_{reac}$ atoms on the substrate surface during transfer of electrons to the substrate.

In this study, the isotopic fractionations produced by DIR are explored over a range in pH and dissolved ion contents to better approximate conditions that existed in ancient marine environments, particularly with regard to dissolved Si, which likely existed in Precambrian oceans at levels approaching saturation with amorphous Si (2.14 mM Si) at ~25 °C (Maliva et al., 2005; Konhauser et al., 2007). We investigated Fe isotope fractionation during hematite reduction by *Geobacter sulfurreducens*, in the presence and absence of dissolved Si, at neutral as well as alkaline pH. Silica polymerization at high pH (e.g., Stumm et al., 1967; Davis et al., 2002) was hypothesized to influence hematite reduction rates, and therefore has potential to affect the quantities of isotopically fractionationated Fe(II) produced by DIR. Moreover, adsorption of Si to hematite may change local bonding environments of reactive Fe(III) on the surface by forming Si–O–Fe bonds (e.g., Schwertmann and Thalmann, 1976; Vempati and Loeppert, 1989; Masion et al., 2001; Doelsch et al., 2003), potentially influencing Fe isotope fractionations. Our results demonstrate that pH and Si may exert strong controls on the rates of reduction, as well as Fe isotope fractionations, but that DIR remains a viable explanation for the large Fe isotope excursions produced in Neoarchean to Paleoproterozoic marine sedimentary record.

2. EXPERIMENTAL DESIGN AND METHODS

2.1. Experimental design

In designing the experiments, our intention was to bridge the gap between the relatively simple conditions used in previous experiments on Fe isotope fractionation during DIR and those that may be closer to those of the Precambrian oceans in several components, including dissolved ions and pH. We examined the effects of dissolved ions using Si, because one of the most dramatic contrasts in seawater chemistry between the Precambrian and Phanerozoic lies in dissolved Si, where Si in the Precambrian oceans may have reached saturated conditions, prior to evolution of Si-secreting organisms in the Phanerozoic (Maliva et al., 2005; Konhauser et al., 2007). We used a dissolved Si content of 2.14 mM, which is close to solubility of amorphous Si in water at 25 °C (Iler, 1979). In addition to conducting experiments in neutral-pH Pipes (1,4-piperazine-N,N′-bis-2-ethanesulfonic acid, sesquisodium salt) buffer, analogous to our previous studies (Crosby et al., 2005, 2007), we performed experiments at pH 8.7, obtained upon addition of 2.14 mM Na_2SiO_3 to neutral-pH Pipes buffer. In the absence of precise knowledge about the pH conditions of Precambrian oceans (see Section 4.3), we chose not to modify this pH value. In addition, this value is closer to that of modern seawater (pH 8.1), and is slightly higher than the point of zero charge for hematite (8.5; e.g., Stumm, 1992; Liger et al., 1999; Jeon et al., 2001), which allows testing of any effects due to negatively ($pH > 8.5$) vs. positively ($pH < 8.5$) charged hematite surfaces.

2.2. Fe(III) oxide substrate

The Fe(III) oxide substrate used in the current study was hematite (α-Fe_2O_3) purchased from Fisher Scientific (Waltham, MA, USA). X-ray diffraction confirmed that the material is hematite, and that no other phases were present. The BET surface area was determined to be 10.8 m^2/g and the particle had an average diameter of 100 nm (determined by TEM). Although hematite is not the most common Fe(III) mineral utilized by iron-reducing bacteria in natural systems (Roden, 2008), it is amenable to partial dissolution by weak HCl as a means for determining the components that have undergone isotopic exchange (Crosby et al., 2005, 2007). In addition, among the various Fe(III) oxides, hematite is the only mineral yet studied where the Fe isotope fractionation factors have been determined in abiologic systems to provide a reference frame for interpreting the fractionations produced in biological systems (see Section 4.2).

2.3. Bacterial strains and culturing

Experiments were performed using the dissimilatory Fe(III)-reducing bacterium *G. sulfurreducens* strain PCA

(Caccavo et al., 1992). *G. sulfurreducens* was grown with fumarate as the electron acceptor, and acetate as the carbon and energy source, prior to inoculation of the hematite-bearing experiments. Cells were harvested and washed twice with sterile, anaerobic Pipes buffer (10 mM, pH 7) before adding ~10^8 cells/mL to 100 mL of sterile, anaerobic, H_2-saturated Pipes buffer containing 50 mM of hematite (100 mM Fe(III)). Eight experiments (four pairs of duplicate reactors) were conducted: with and without 2.14 mM Si (added as $Na_2SiO_3{\cdot}9H_2O$) at pH 7, and with and without 2.14 mM Si at pH 8.7. H_2 served as the only energy source for Fe(III) reduction. The ionic strength of all the media was about 0.02 M. Non-growth conditions (no added C, N, or P) were employed to avoid precipitation of carbonate- and phosphate-containing Fe minerals, which could complicate interpretation of the Fe isotope data. The bottles were incubated at 30 °C in the dark, and all sampling and extraction was carried out inside an anaerobic chamber (Coy Products, Grass Lake, MI, USA).

2.4. Sampling and extraction procedures

Aliquots (10 mL) of the hematite suspensions were collected periodically over the course of 60 days and centrifuged (under N_2 in gas-tight plastic centrifuge tubes) to isolate the aqueous fraction. The remaining solids were extracted for 10 min with 0.05 M HCl to remove the majority of sorbed Fe(II) (defined as $Fe(II)_{sorb}$) without dissolving any underlying Fe(III); the lack of dissolution of any Fe(III) oxide in this step was confirmed through Fe(II) and total Fe measurements. Fe(II) and total Fe concentrations were measured using *Ferrozine* (Stookey, 1970) with and without hydroxylamine-HCl, and Fe(III) was determined by difference. A second extraction was performed using 0.5 M HCl for ~18 h to remove any remaining $Fe(II)_{sorb}$, and to dissolve a small amount of Fe(III) oxide. All samples were passed through 0.2 μm filters to avoid carryover of hematite particles, and aqueous and 0.05 M HCl fractions were acidified with HCl to a final concentration of ~0.5 M to stabilize dissolved Fe. Silica concentrations in aqueous phase samples and HCl extracts were measured using an ICP-OES.

2.5. Abiologic Fe–Si gel experiments

In order to gain insight into potential Fe isotope effects through formation of Fe(II)–Si gel in the pH 8.7 Si added experiments, we conducted abiologic experiments in the absence of hematite. $FeCl_2$ (0.5 mM) with an initial $\delta^{56}Fe$ value of −0.52‰ was added to 10 mL of 10 mM anaerobic Pipes buffer containing 2.14 mM Si at pH 8.7. The bottles were agitated either once during sampling or constantly on a roller table, as noted in the data table. After 8 days, samples were centrifuged to remove Fe(II)–Si gel from aqueous fraction. The supernatant was passed through a 0.2 μm filter. The Fe–Si gel pellet was dissolved using 0.5 M HCl. One milliliter of 0.5 M HCl was then added to the bottle in order to retrieve residue attached to the bottle wall. Finally, the filter paper was collected and dissolved in 7 M HCl to completely recover added Fe. Concentrations of Fe and Si in different fractions were measured as described above.

2.6. Fe isotope measurements and control tests

All Fe-containing solutions including 14 synthetic solutions were purified using anion-exchange chromatography (typical column yields 98%), followed by Fe isotope measurements using a MC-ICP-MS, as previously described (Beard et al., 2003). $Fe(II)_{aq}$ fractions from pH 8.7 experiments were not analyzed for isotopic compositions due to their very low Fe contents (<10 μg). Data are reported as $^{56}Fe/^{54}Fe$ ratios relative to the average of igneous rocks in standard δ notation, in units of per mil (‰):

$$\delta^{56}Fe = \left[\frac{^{56}Fe/^{54}Fe_{sample}}{^{56}Fe/^{54}Fe_{IgRxs}} - 1\right] \times 10^3 \quad (1)$$

Data are also reported as $\delta^{57}Fe$ values, based on the $^{57}Fe/^{54}Fe$ ratio, defined in an analogous manner. Measured external precision in $\delta^{56}Fe$ values is ±0.08‰, which is two standard deviations (2σ) based on replicate standard analyses ($n = 112$). On the igneous rock scale, the $\delta^{56}Fe$ value of the IRMM-014 standard is −0.09‰ (Beard et al., 2003). The Fe isotope fractionation between two phases or species A and B is defined as:

$$\Delta^{56}Fe_{A-B} = \delta^{56}Fe_A - \delta^{56}Fe_B \quad (2)$$

following standard practice.

To check that the hematite used as a substrate was isotopically homogeneous, several partial dissolutions were done using 3 M HCl for varying lengths of time. Complete dissolution of bulk samples using 7 M HCl indicated that the initial $\delta^{56}Fe$ value of the hematite was +0.13‰ (Table 1). All of the partial dissolution tests indicated that the hematite is isotopically homogenous within analytical uncertainty (Table 1).

Table 1
Initial Fe isotope compositions of hematite and tests for isotopic homogeneity.

Sample	Aliquot[a]	Analyses			
		$\delta^{56}Fe$	2-SE[b]	$\delta^{57}Fe$	2-SE[b]
Hematite starting material					
	1	0.12	0.02	0.18	0.02
	2	0.15	0.02	0.21	0.02
Hematite partial dissolution					
1.7% dissolved	Aqueous	0.21	0.03	0.31	0.03
1.7% dissolved	Solids	0.10	0.03	0.17	0.02
8.6% dissolved	Aqueous	0.13	0.02	0.24	0.02
8.6% dissolved	Solids	0.11	0.02	0.16	0.02
17.0% dissolved	Aqueous	0.16	0.02	0.26	0.02
17.0% dissolved	Solids	0.08	0.03	0.15	0.02
23.4% dissolved	Aqueous	0.16	0.03	0.23	0.02
23.4% dissolved	Solids	0.11	0.02	0.14	0.02

[a] Different aliquots are from the same sample but were separately processed through anion-exchange chromatography.
[b] 2-SE is the internal standard error based on forty 10-s on-peak integrations taken for each analysis.

Accuracy of Fe isotope results were evaluated by analysis of 14 synthetic solutions that consisted of 5 mL of 10 mM Pipes with 2.4–8.0 μg of Fe of known isotopic composition added to them. The average δ^{56}Fe value of these synthetic solutions was 0.46 ± 0.14 (2σ; $n = 14$), which is identical to the isotope composition measured for the pure Fe solution ($\delta^{56}Fe = 0.46 \pm 0.08$; 2σ; $n = 36$).

3. RESULTS

We first compare hematite reduction rates as a function of pH and the presence and absence of Si. Differences among the biological experiments in their Fe isotope compositions and proportions of Fe species are then presented, followed by results from Fe–Si gel experiments.

3.1. Comparison of hematite reduction at pH 7 and pH 8.7, with and without Si

Over the course of 60 days, only a small fraction of hematite (<1%) was reduced under the experimental conditions (Fig. 2, electronic annex Tables EA1–4). The extent of hematite reduction was ~10-fold lower at elevated pH in the presence of Si (Fig. 2A and C). The pH effect was smaller (~2-fold) but still significant in the absence of Si (Fig. 2B and D). Total recovery of Si was attained when the Si contents of the aqueous aliquot and 0.05 M HCl and 0.5 M HCl extracts were summed (Fig. 3, Table 2). This observation excludes the possibility that Fe(II) was sequestered in acid-insoluble iron-silicates, which may occur at high pH (Klein, 2005). The low total Fe(II) contents at pH 8.7 in the presence of Si, therefore, reflects significantly decreased hematite reduction by *G. sulfurreducens*, rather than production of an Fe(II) phase that was not sampled. Total Fe(II) decreased slightly after 40 or 51 days in three of the four experiments, but this did not correlate with changes in Si contents within measurement uncertainties (Fig. 3). The strong decrease in total Fe(II) at day 60 in the pH 8.7 no Si experiment was likely due to incomplete homogenization of the hematite suspension during sampling at the last time point.

$Fe(II)_{aq}$ and 0.05 M HCl-extractable $Fe(II)_{sorb}$ comprised the majority of total Fe(II) at pH 7, regardless of the presence or absence of Si (Fig. 2A and B). The amount of $Fe(II)_{aq}$ was much smaller at pH 8.7 (Fig. 2C and D), and $Fe(II)_{sorb}$ extracted with 0.05 M HCl was the major component of total Fe(II). This result is consistent with increased sorption of Fe(II) to hematite surfaces when pH is increased (e.g., Liger et al., 1999; Jeon et al., 2001; Strathmann and Stone, 2003). The 0.05 M HCl extraction recovered exclusively Fe(II), whereas 0.5 M HCl extractions removed a mixture of Fe(II) and Fe(III). Most of the 0.5 M HCl extracts, except for those from the initial time point, were predominately composed of Fe(III), with Fe(III)/total Fe ratios >0.6 (Tables EA1–4).

3.2. Fe isotope exchange during hematite reduction

The δ^{56}Fe values of $Fe(II)_{aq}$ ($\delta^{56}Fe_{Fe(II)aq}$) and $Fe(II)_{sorb}$ ($\delta^{56}Fe_{Fe(II)sorb}$) varied little over time in Si free medium (Fig. 4B and D), and were ~1.3‰ and ~0.9‰ lower than the initial hematite substrate, respectively (Fig. 4B). These results are consistent with previous studies of bacterial hematite reduction without Si (Crosby et al., 2005, 2007).

$\delta^{56}Fe_{Fe(II)aq}$ and $\delta^{56}Fe_{Fe(II)sorb}$ increased gradually over time in the pH 7 Si added experiment (Fig. 4A), whereas at pH 8.7, $\delta^{56}Fe_{Fe(II)sorb}$ decreased by ~0.5‰ (Fig. 4C). $\delta^{56}Fe_{Fe(II)aq}$ and $\delta^{56}Fe_{Fe(II)sorb}$ values were ~0.5–1.0‰

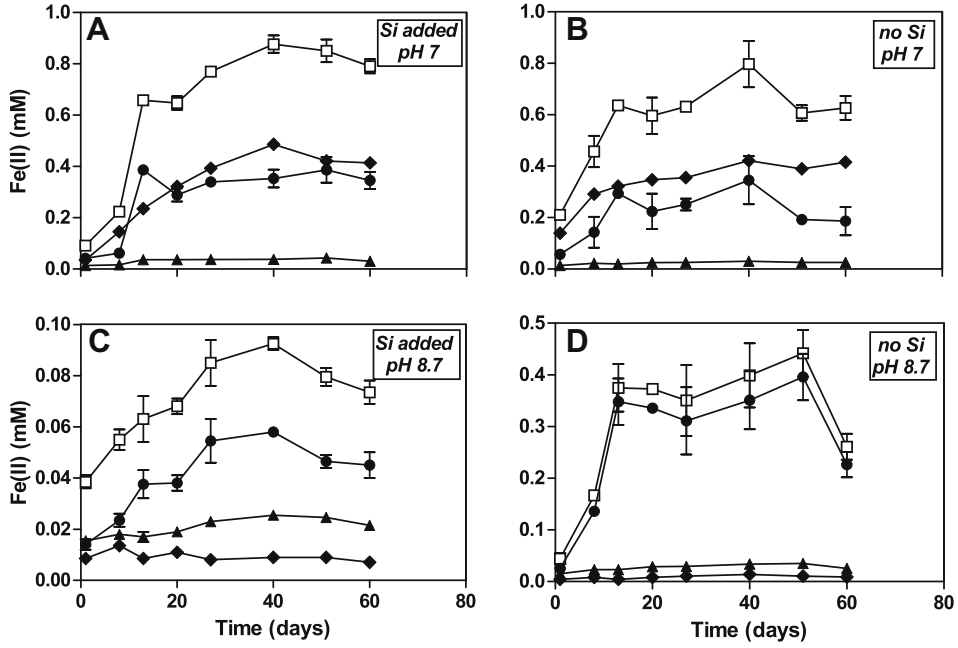

Fig. 2. Hematite reduction by *Geobacter sulfurreducens* in the presence of dissolved Si (2.14 mM Si) at pH 7 (A) and 8.7 (C), and in the absence of Si at pH 7 (B) and 8.7 (D). ♦ = $Fe(II)_{aq}$; ● = $Fe(II)_{sorb}$ in 0.05 M HCl extract; ▲ = $Fe(II)_{sorb}$ in 0.5 M HCl extract; □ = Total Fe(II) (sum of $Fe(II)_{aq}$ and $Fe(II)_{sorb}$ in the 0.05 M and 0.5 M HCl extracts). Error bars show the range of duplicate suspensions.

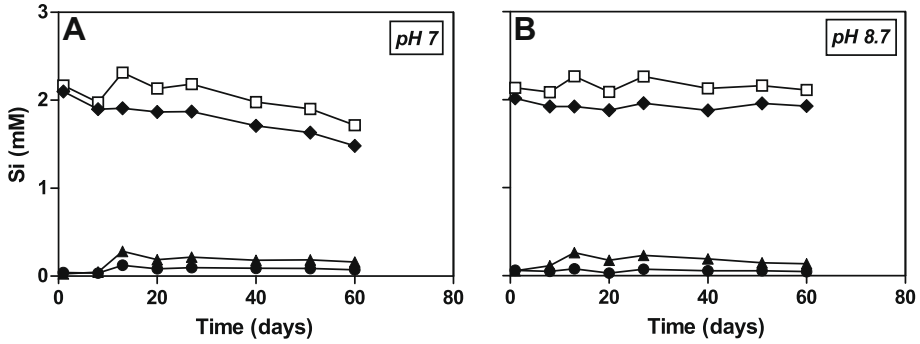

Fig. 3. Temporal variations in Si concentrations for experiments at pH 7 (A) and pH 8.7 (B). ♦ = aqueous Si; ● = Si in 0.05 M HCl extract; ▲ = Si in 0.5 M HCl extract; □ = Total Si (sum of aqueous Si and Si in the 0.05 M and 0.5 M HCl extracts).

Table 2
Dissolved Si and Fe(II) concentrations of aqueous, 0.05 M HCl and 0.5 M HCl extracts and Si:Fe ratios for experiments at pH 7 and pH 8.7.

Experiments	Replicate	Day	Aqueous		0.05 M HCl			0.5 M HCl		
			Si (mM)	Fe(II) (mM)	Si (mM)	Fe(II) (mM)	Si:Fe	Si (mM)	Fe(II) (mM)	Si:Fe[a]
pH 7	1	1	2.109	0.037	0.038	0.031	1.2	0.021	0.013	1.3
	2	1	2.088	0.034	0.047	0.053	0.9	0.033	0.015	1.2
	1	8	1.897	0.146	0.024	0.044	0.5	0.032	0.016	0.9
	2	8	1.898	0.145	0.043	0.080	0.5	0.058	0.017	1.0
	1	13	1.907	0.231	0.123	0.392	0.3	0.282	0.038	0.9
	2	13	1.910	0.240	0.122	0.381	0.3	0.280	0.034	1.0
	1	20	1.872	0.321	0.089	0.315	0.3	0.210	0.036	0.9
	2	20	1.860	0.323	0.077	0.263	0.3	0.162	0.036	0.8
	1	27	1.886	0.392	0.095	0.344	0.3	0.226	0.039	0.8
	2	27	1.856	0.394	0.097	0.335	0.3	0.207	0.035	0.8
	1	40	1.715	0.481	0.106	0.388	0.3	0.199	0.041	0.7
	2	40	1.701	0.491	0.073	0.318	0.2	0.164	0.034	0.7
	1	51	1.639	0.424	0.078	0.337	0.2	0.158	0.045	0.6
	2	51	1.623	0.419	0.096	0.436	0.2	0.210	0.040	0.6
	1	60	1.471	0.423	0.065	0.312	0.2	0.151	0.028	0.6
	2	60	1.489	0.405	0.080	0.379	0.2	0.174	0.033	0.6
pH 8.7	1	1	2.008	0.009	0.052	0.012	4.3	0.039	0.015	3.4
	2	1	2.027	0.008	0.072	0.016	4.4	0.073	0.016	4.5
	1	8	1.956	0.014	0.039	0.021	1.9	0.079	0.017	3.1
	2	8	1.889	0.013	0.057	0.026	2.2	0.150	0.019	4.6
	1	13	1.918	0.010	0.087	0.043	2.0	0.292	0.019	6.2
	2	13	1.931	0.007	0.073	0.032	2.3	0.233	0.015	6.6
	1	20	1.834	0.011	0.029	0.041	0.7	0.180	0.019	3.5
	2	20	1.931	0.011	0.031	0.035	0.9	0.170	0.019	3.7
	1	27	1.947	0.008	0.079	0.063	1.3	0.265	0.023	4.0
	2	27	1.973	0.008	0.068	0.046	1.5	0.196	0.023	3.8
	1	40	1.871	0.009	0.052	0.059	0.9	0.186	0.027	2.8
	2	40	1.888	0.009	0.062	0.057	1.1	0.199	0.024	3.2.
	1	51	1.945	0.009	0.053	0.044	1.2	0.133	0.023	2.8
	2	51	1.972	0.009	0.058	0.049	1.2	0.161	0.026	2.9
	1	60	1.901	0.007	0.048	0.050	1.0	0.150	0.021	2.8
	2	60	1.955	0.007	0.045	0.040	1.1	0.122	0.022	2.7

[a] Si:Fe ratios were combined Si in 0.05 M HCl and 0.5 M HCl extracts versus total sorbed Fe(II) (equal to Fe(II) in 0.05 M HCl extract plus Fe(II) in 0.5 M HCl extract).

and ~0.4–0.7‰ lower than the initial hematite, respectively, at pH 7 (Fig. 4A). $\delta^{56}Fe_{Fe(II)sorb}$ averaged ~1.2‰ lower than the initial hematite at pH 8.7 (Fig. 4C). At all time points the δ^{56}Fe values of the 0.5 M HCl extracts were similar to or greater than the initial hematite substrate, indicating that isotopically heavy $Fe(III)_{reac}$ formed at the hematite surface through isotopic exchange with $Fe(II)_{aq}$ and $Fe(II)_{sorb}$.

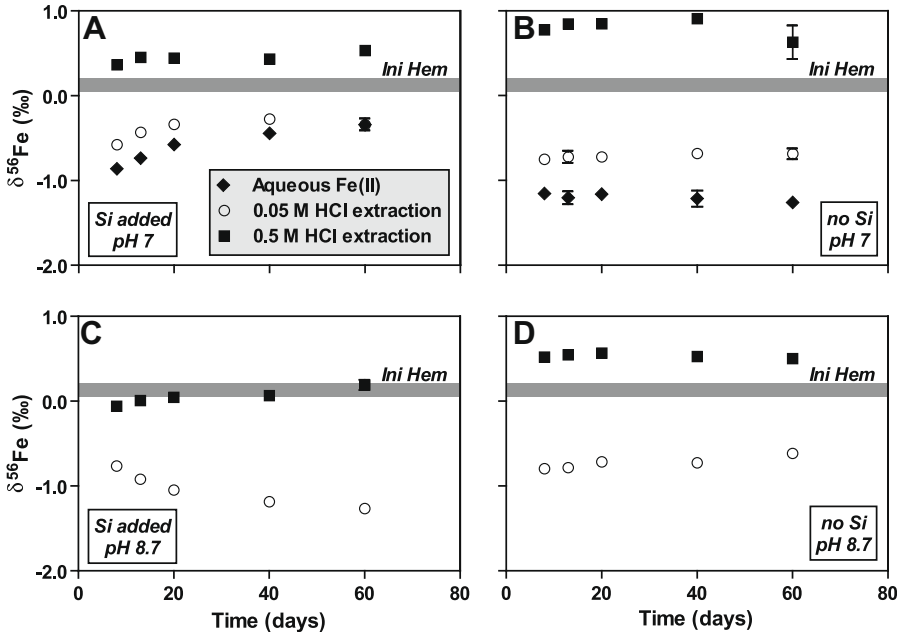

Fig. 4. Temporal changes in $\delta^{56}Fe$ values for $Fe(II)_{aq}$, 0.05 M HCl-extractable $Fe(II)_{sorb}$, and total Fe (both Fe(II) and Fe(III)) in the 0.5 M HCl extract. Errors are smaller than the symbol size unless otherwise indicated. Error bars show the range of duplicate suspensions. The horizontal bars show the initial Fe isotope composition of the hematite substrate.

3.3. Calculation of $\delta^{56}Fe$ values for the Fe(III) end-member in the 0.5 M HCl extracts

Following Crosby et al. (2005, 2007), we may assume that the bulk Fe isotope composition of 0.5 M HCl extracts are a mixture of Fe(II) and $Fe(III)_{reac,}$ where Fe(II) reflects $Fe(II)_{sorb}$ not recovered by the 0.05 M HCl extraction, and $Fe(III)_{reac}$ is a reactive Fe(III) component on the hematite surface that was open to isotopic exchange. We assume that the $\delta^{56}Fe$ values of the Fe(II) component are the same as $Fe(II)_{sorb}$ recovered by the 0.05 M HCl extraction; this assumption is supported by the observation of consistent isotopic fractionations over a range of $Fe(II)_{aq}$ and $Fe(II)_{sorb}$ contents (Crosby et al., 2007). This approach allows calculation of the $\delta^{56}Fe$ value of the $Fe(III)_{reac}$ component of the 0.5 M HCl extracts ($\delta^{56}Fe_{Fe(III)reac}$) using a simple isotopic mass balance equation (Crosby et al., 2007):

$$\delta^{56}Fe_{0.5\ M\ HCl} = X_{Fe(II)}\delta^{56}Fe_{Fe(II)sorb} + X_{Fe(III)}\delta^{56}Fe_{Fe(III)reac} \quad (3)$$

where X represents the mole fractions of Fe(II) and Fe(III) in the 0.5 M HCl extract. $X_{Fe(II)}$ and $\delta^{56}Fe_{0.5\ M\ HCl}$ from this mass-balance relation are plotted in Fig. 5 for each of the four experiments. In addition, $\delta^{56}Fe_{Fe(II)sorb}$ is plotted at $X_{Fe(II)} = 1.0$, and with these additional points, a mixing line was constructed for each time point to calculate the $\delta^{56}Fe$ values for the pure Fe(III) component (where $X_{Fe(II)} = 0$).

The most precise estimates of $\delta^{56}Fe_{Fe(III)reac}$ are obtained for 0.5 M HCl extracts that have high proportions of Fe(III). The Excel add-in ISOPLOT (Ludwig, 1991) was used to calculate the 2σ errors in $\delta^{56}Fe_{Fe(III)reac}$, incorporating uncertainties for *Ferrozine* measurement and measured isotopic compositions. Because the 0.5 M HCl extracts for the two duplicate reactors contain different proportions of Fe(II) and Fe(III), each of the two duplicates was calculated individually to obtain its $\delta^{56}Fe_{Fe(III)reac}$ and 2σ error using ISOPLOT (Fig. 5), and the average was taken and errors were propagated for the average. All 0.5 M HCl extracts had more than 40% of Fe(III), and most had greater than 60% Fe(III). The calculated errors for $\delta^{56}Fe_{Fe(III)reac}$ were $<0.4‰$ for extracts with <60% Fe(III) and $<0.2‰$ for extracts with >60% Fe(III). Calculated $\delta^{56}Fe_{Fe(III)reac}$ values for the Si added experiments ranged from $+0.8‰$ to $+1.9‰$ at pH 7, and $+0.2‰$ to $+1.5‰$ at pH 8.7 (Fig. 5A and C). For the no Si experiments, the $\delta^{56}Fe_{Fe(III)reac}$ values ranged from $+1.2‰$ to $+1.8‰$ at pH 7 and $+0.7‰$ to $+1.3‰$ at pH 8.7 (Fig. 5B and D). All of these $\delta^{56}Fe_{Fe(III)reac}$ values were significantly higher than that of the initial hematite.

3.4. Isotopic fractionations among $Fe(II)_{aq}$–$Fe(II)_{sorb}$–$Fe(III)_{reac}$ at pH 7 and 8.7

The $\Delta^{56}Fe_{Fe(II)aq-Fe(II)sorb}$ fractionation was invariant throughout the pH 7 experiments, for which the weighted average (calculated using ISOPLOT) values were $-0.20 \pm 0.16‰$ and $-0.49 \pm 0.09‰$, respectively, for the no Si and plus Si systems (Fig. 6). In comparison, Crosby et al. (2007) measured the values of $-0.30 \pm 0.08‰$ for bacterial reduction of hematite at pH 7 in the absence of Si (Fig. 6B). The reason for the small difference between this study and Crosby et al. (2007) is unknown but may reflect the more efficient recovery of $Fe(II)_{sorb}$ using 0.05 M HCl compared to sodium acetate.

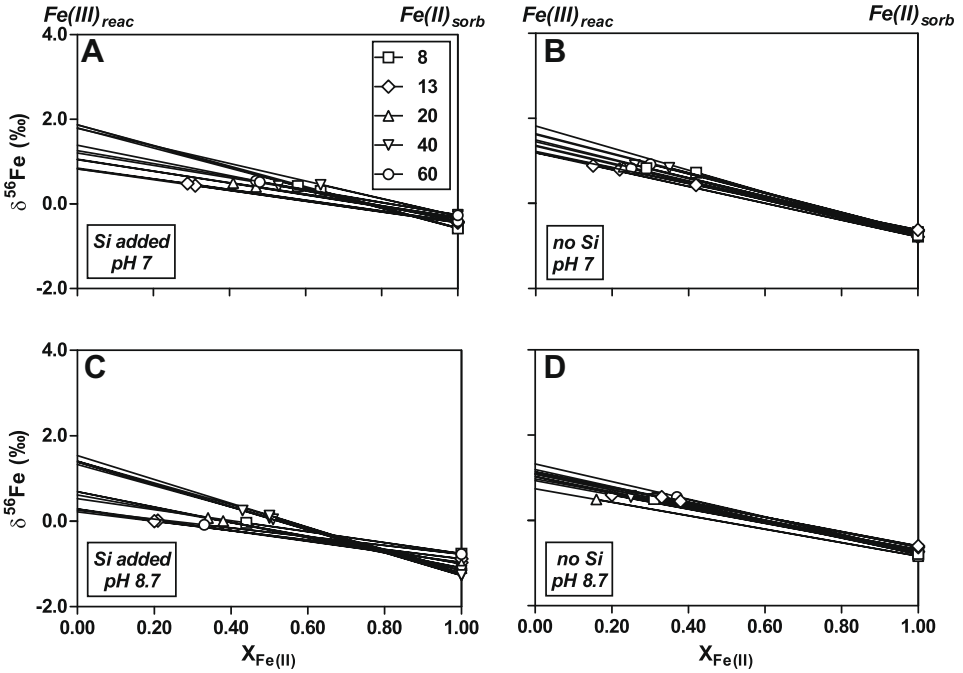

Fig. 5. Mixing diagrams illustrating calculation of Fe(III) end-member component in the 0.5 M HCl extracts, which contained mixtures of Fe(II) and Fe(III). δ^{56}Fe–$X_{Fe(II)}$ pairs for each time point (days shown in legend) reflect those measured in the 0.5 M HCl extract ($X_{Fe(II)} < 1.0$) or in the 0.05 M HCl extract ($X_{Fe(II)} \equiv 1.0$). Extraploation from $X_{Fe(II)} = 1.0$ and $\delta^{56}Fe_{Fe(II)sorb}$, through the δ^{56}Fe and $X_{Fe(II)}$ measured for the 0.5 M HCl extract, to $X_{Fe(II)} = 0.0$ allows calculation of the δ^{56}Fe values for the pure Fe(III) component in the extract.

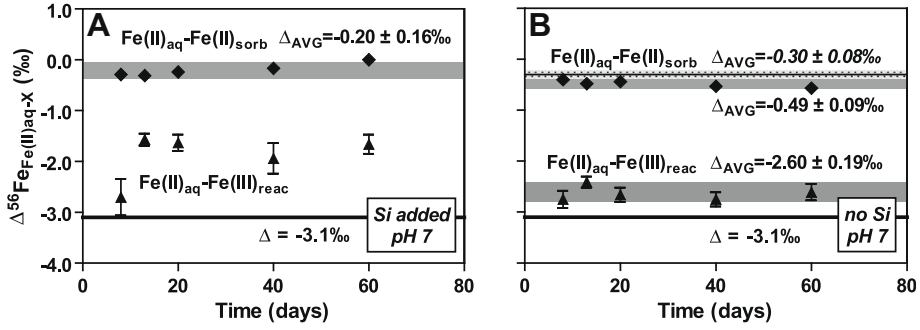

Fig. 6. Temporal variations in $Fe(II)_{aq}$–$Fe(II)_{sorb}$ (♦) and $Fe(II)_{aq}$–$Fe(III)_{reac}$ (▲) isotope fractionation factors for experiments at pH 7 in the presence of Si (A) and absence of Si (B). Error bars for each time point reflect 2σ uncertainties propagated from errors in measured δ^{56}Fe values for $Fe(II)_{aq}$ and $Fe(II)_{sorb}$, and calculated uncertainties in $\delta^{56}Fe_{Fe(III)reac}$ based on errors in the extrapolations shown in Fig. 5. Gray horizontal bars show weighted averages for each fractionation factor from this study. Dotted horizontal bars show weighted average for $Fe(II)_{aq}$–$Fe(II)_{sorb}$ fractionation factor from Crosby et al. (2007; Δ_{AVG} is shown in italics). Black horizontal lines indicate $Fe(II)_{aq}$–$Fe(III)_{reac}$ fractionation factor for the system Fe(II)–hematite. The $Fe(II)_{aq}$–$Fe(III)_{reac}$ fractionation factor for Si added pH 7 experiments deviated from that of the system Fe(II)–hematite, reflecting involvement of an $Fe(III)_{reac}$ component that is not hematite.

The $\Delta^{56}Fe_{Fe(II)aq–Fe(III)reac}$ fractionation also showed little variation with time in the pH 7 no Si experiments (Fig. 6B). The mean fractionation of $-2.60 \pm 0.19‰$ was slightly smaller than that measured by Crosby et al. (2007) ($-2.95 \pm 0.19‰$), although these fractionations overlap within error. In the pH 7 Si added experiment, the $\Delta^{56}Fe_{Fe(II)aq–Fe(III)reac}$ fractionation was $-2.70 \pm 0.36‰$ at day 8, which was comparable to the average fractionation measured in the no Si experiment. The $\Delta^{56}Fe_{Fe(II)aq–Fe(III)reac}$ fractionation decreased after day 8 to a constant value of $-1.64 \pm 0.18‰$ (Fig. 6A). This is a markedly different fractionation than any yet measured during bacterial reduction of hematite.

Almost the entire Fe(II) inventory existed as $Fe(II)_{sorb}$ at pH 8.7 (Fig. 2), preventing accurate measurement of $\delta^{56}Fe_{Fe(II)aq}$. We therefore cast isotopic fractionations with $Fe(III)_{reac}$ relative to $Fe(II)_{sorb}$ and compare these to values obtained in the pH 7 experiments (Fig. 7). The $\Delta^{56}Fe_{Fe(II)sorb–Fe(III)reac}$ fractionation was $-1.76 \pm 0.21‰$ for the pH 8.7 no Si experiment (Fig. 7D). This value overlaps with that of $-2.11 \pm 0.21‰$ for the pH 7 no Si experiment (Fig. 7B). In both of these experiments,

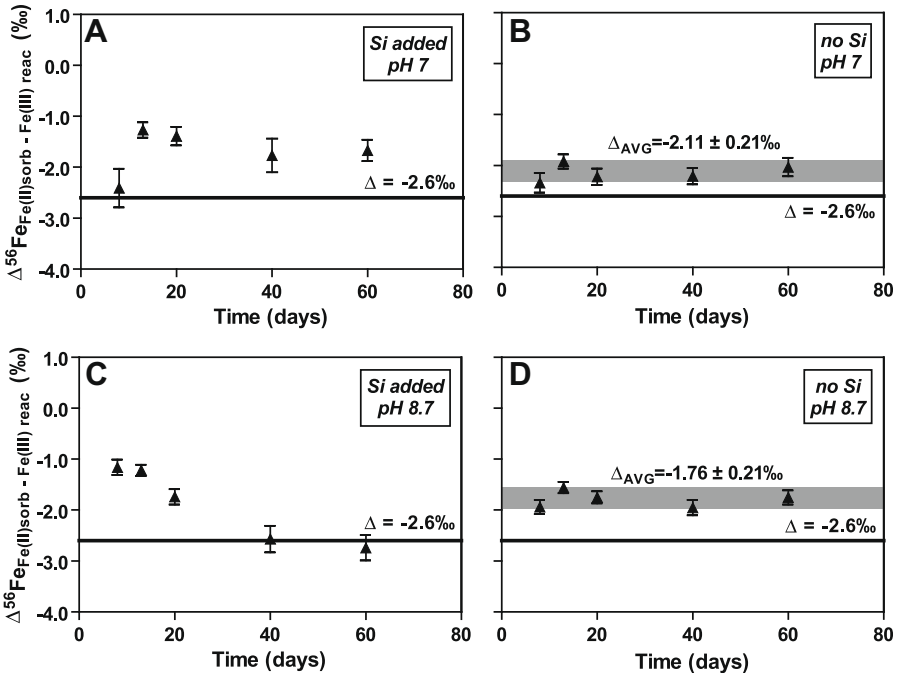

Fig. 7. Temporal variations in $Fe(II)_{sorb}$–$Fe(III)_{reac}$ isotope fractionation factors for pH 7 Si added (A), pH 7 no Si (B), pH 8.7 Si added (C), and pH 8.7 no Si (D) experiments. Error bars for each time point reflect 2σ uncertainties propagated from errors in measured $\delta^{56}Fe_{Fe(II)sorb}$ values and calculated uncertainties in $\delta^{56}Fe_{Fe(III)reac}$ based on errors in the extrapolations shown in Fig. 5. Gray horizontal bars show weighted averages for each fractionation factor from this study for silica-absent experiments. Black horizontal lines indicate $Fe(II)_{sorb}$–$Fe(III)_{reac}$ fractionation factor for the system Fe(II)–hematite. The $Fe(II)_{sorb}$–$Fe(III)_{reac}$ fractionation factors for silica-bearing experiments deviated from that of the system Fe(II)–hematite, reflecting involvement of an $Fe(III)_{reac}$ component that is not hematite, such as a Fe–O–Si polymer on the surface of the hematite substrate.

$\Delta^{56}Fe_{Fe(II)sorb–Fe(III)reac}$ values did not systematically vary with time. In contrast, $\Delta^{56}Fe_{Fe(II)sorb–Fe(III)reac}$ fractionations varied with time in the Si added experiments, particularly at high pH (Fig. 7A and C). In the pH 7 experiment, the fractionation was $-2.41 \pm 0.38‰$ at day 8 and then decreased to an average of $-1.43 \pm 0.34‰$ that remained constant (Fig. 7A). In the pH 8.7 experiment, the fractionation was approximately $-1.2‰$ at day 8 and day 13, and then increased to $-1.74 \pm 0.15‰$ at day 20; the last two time points averaged $-2.66 \pm 0.18‰$ (Fig. 7C).

3.5. Proportions of $Fe(II)_{aq}$, $Fe(II)_{sorb}$, and $Fe(III)_{reac}$ in the reactive Fe pool

The mole sum of $Fe(II)_{aq}$, $Fe(II)_{sorb}$, and $Fe(III)_{reac}$ comprises the total reactive Fe pool ($M_{TOT\ ReacFe}$) that underwent isotopic exchange (Fig. 1), and this pool must have the same isotopic composition as the starting hematite substrate (Crosby et al., 2005). In our experiments, the moles of $Fe(II)_{aq}$ ($M_{Fe(II)aq}$) are determined by the measured concentrations and the volume of $Fe(II)_{aq}$. The moles of $Fe(II)_{sorb}$ ($M_{Fe(II)sorb}$) are the sum of Fe(II) measured in the 0.05 M HCl and 0.5 M HCl extracts. The moles of $Fe(III)_{reac}$ ($M_{Fe(III)reac}$) cannot be directly measured but can be calculated based on isotopic mass balance constraints as follows (Crosby et al., 2007):

$$M_{TOT\ ReacFe} = \frac{\delta^{56}Fe_{Fe(II)aq} \cdot M_{Fe(II)aq} + \delta^{56}Fe_{Fe(II)sorb} \cdot M_{Fe(II)sorb} + \delta^{56}Fe_{Fe(III)reac} \cdot M_{Fe(III)reac}}{\delta^{56}Fe_{Sys}} = M_{Fe(II)aq} + M_{Fe(II)sorb} + M_{Fe(III)reac} \quad (4)$$

In order to make direct comparisons with previous isotopic studies, we normalize to a system Fe isotope composition of $\delta^{56}Fe_{Sys} = 0$ by subtracting $+0.13‰$ from all measured $\delta^{56}Fe$ values, as well as the initial calculated $\delta^{56}Fe_{Fe(III)reac}$ value. Solving Eq. (4) for $M_{Fe(III)reac}$ produces the relation:

$$M_{Fe(III)reac} = \frac{-\delta^{56}Fe_{Fe(II)aq} \cdot M_{Fe(II)aq} - \delta^{56}Fe_{Fe(II)sorb} \cdot M_{Fe(II)sorb}}{\delta^{56}Fe_{Fe(III)reac}} \quad (5)$$

Note here that $M_{Fe(III)reac}$ is the amount of Fe(III) in hematite that is required to attain isotopic mass balance among

$Fe(II)_{aq}$, $Fe(II)_{sorb}$, and $Fe(III)_{reac}$; $M_{Fe(III)reac}$ is not equal to the measured Fe(III) in the 0.5 M HCl extract. It is important to note that the calculated amount of $M_{Fe(III)reac}$ based on isotopic mass balance (Eq. (5)) were always greater than the moles of Fe(III) measured in the 0.5 M HCl extract, which indicates that none of the original unreacted hematite substrate was dissolved in the 0.5 M HCl extracts. This is critical, because if the 0.5 M HCl extract contained Fe(III) from the original hematite, the effect would be to produce anomalously low fractionations, which would affect our conclusions.

Crosby et al. (2007) adopted an alternative to Eq. (5) by recasting $\delta^{56}Fe_{Fe(III)reac}$ in terms of the mean $\Delta^{56}Fe_{Fe(II)aq–Fe(III)reac}$ fractionation that was measured for all time points. This approach was used to minimize error propagations that were associated with sometimes large uncertainties in the individually calculated $\delta^{56}Fe_{Fe(III)reac}$ values for each sample because Fe(II) contents in their 0.5 M HCl extracts were often high, requiring a large extrapolation to the pure Fe(III) end-member (Fig. 5). In this study we do not assume a constant $\Delta^{56}Fe_{Fe(II)aq–Fe(III)reac}$ because (1) there does not appear to be a constant $\Delta^{56}Fe_{Fe(II)aq–Fe(III)reac}$ fractionation that is applicable to all samples and (2) we obtained higher proportions of Fe(III) in our 0.5 M HCl extracts (typically >60%) relative to that of Crosby et al. (2007) due to longer extraction time with 0.5 M HCl (~18 h vs. 1 h). We therefore use Eq. (5) to calculate the moles of $Fe(III)_{reac}$ because we were able to infer a precise $\delta^{56}Fe$ value for the $Fe(III)_{reac}$ component. For pH 8.7 experiments, the $\delta^{56}Fe_{Fe(II)aq}$ values are calculated assuming that the average $\Delta^{56}Fe_{Fe(II)aq–Fe(II)sorb}$ fractionations for the systems with and without Si are the same as those at pH 7, equal to −0.20‰ and −0.49‰, respectively. This assumption is required because $\delta^{56}Fe_{Fe(II)aq}$ was not directly measured in the pH 8.7 experiments, but introduces negligible error in Eq. (5) due to the very small quantities of $Fe(II)_{aq}$ in these experiments (Fig. 2C and D).

The molar quantities of $Fe(II)_{aq}$, $Fe(II)_{sorb}$, and $Fe(III)_{reac}$, as well as the total reactive Fe pool, are summarized in Table 3. A key result is that increased pH reduced the size of the total reactive Fe pool, regardless of the presence of Si, commensurate with the lower extent of hematite reduction; this in turn led directly to a reduction in the moles of the $Fe(III)_{reac}$. Temporally, in the pH 7 experiments, the total amount of reactive Fe increased from day 8 to day 13 and then leveled off, regardless of the presence of Si. In the pH 8.7 Si added experiments, the size of the reactive Fe pool decreased rapidly after reaching a peak at day 13. In comparison, in the pH 8.7 no Si experiments, the size of the reactive Fe pool did not significantly change from day 13 to day 40, but decreased about half at day 60, which, as noted earlier, likely reflects a sampling error at the last time point.

The relative proportions of $Fe(II)_{aq}$, $Fe(II)_{sorb}$, and $Fe(III)_{reac}$ ($X_{Fe(II)aq}$, $X_{Fe(II)sorb}$, $X_{Fe(III)reac}$) did not significantly change with time at pH 7, regardless of the presence of Si (Fig. 8A). They also remained relatively constant over time at pH 8.7 in the absence of Si (Fig. 8B). In contrast, the proportions changed significantly over time at pH 8.7 in the presence of Si (Fig. 8B). $X_{Fe(III)reac}$ increased slightly from day 8 to day 13, then decreased dramatically to a constant value at the end of the experiment. These variations were accompanied by complementary variations in $X_{Fe(II)sorb}$.

3.6. Fe isotope fractionations upon formation of Fe–Si gel

Although we found no evidence for formation of Fe-silicate minerals using XRD, the very low $Fe(II)_{aq}$ contents in the pH 8.7 Si added experiments raised the possibility that an Fe(II)–Si gel formed that was sampled in the 0.05 M and 0.5 M HCl extractions (Fig. 3, Table EA-3). The potential Fe isotope effects of this phenomenon were investigated in abiologic experiments in the absence of hematite (Table 4). These experiments demonstrated that Fe(II)-rich Si gels may form at pH 8.7. The measured fractionation factor between aqueous Fe(II) and Fe–Si gel was $-0.51 \pm 0.18‰$, which is indistinguishable from the average $\Delta^{56}Fe_{Fe(II)aq–Fe(II)sorb}$ fractionation at pH 7 (Fig. 6). The exact composition of residues in the bottles and on the filter papers remains unknown, but possibilities include some Fe hydroxides and Si polymers. The fact that the $\Delta^{56}Fe_{Fe(II)aq\text{-}Fe–Si\ gel}$ fractionation is indistinguishable from the $\Delta^{56}Fe_{Fe(II)aq–Fe(II)sorb}$ fractionation demonstrates that Fe(II) in the Fe–Si gel will essentially have the same Fe isotope composition as sorbed Fe(II), and thus have no influence on the $\Delta^{56}Fe_{Fe(II)sorb–Fe(III)reac}$ fractionation in the pH 8.7 Si added experiments. This important conclusion allows us to directly compare $\Delta^{56}Fe_{Fe(II)sorb–Fe(III)reac}$ fractionations across all experiments.

4. DISCUSSION

Our experiments demonstrate significant changes in reduction rates and isotopic fractionations as a function of pH and Si. Below we discuss possible mechanisms responsible for the variable reduction rates, as well as differences in Fe bonding environments that may explain the differences in isotopic fractionations relative to pure Fe(II)/hematite systems. Finally, we discuss the applicability of our experiments to marine environments in the Precambrian.

4.1. Effect of pH and Si on hematite reduction

Hematite reduction by *G. sulfurreducens* was inhibited at elevated pH, dramatically so in the presence of Si. It has been shown that accumulation of biogenic Fe(II) on Fe(III) oxide and Fe(III)-reducing bacterial cell surfaces governs the extent of crystalline Fe(III) oxides reduction through blockage of active surface sites (e.g., Urrutia et al., 1998; Roden and Urrutia, 1999, 2002; Roden, 2004). At alkaline pH, Fe(II) existed exclusively as sorbed Fe(II) and the amount of $Fe(II)_{sorb}$ was, in fact, comparable to that at pH 7 (Fig. 2). A decline in the total extent of hematite reduction at high pH can therefore be explained by the absence of $Fe(II)_{aq}$ accumulation and associated rapid blockage of active surface sites by $Fe(II)_{sorb}$. The dramatic effect of Si at alkaline pH may be similarly attributed to sorption (or precipitation) of Si onto hematite surfaces, further reducing the number of surface sites available for bacterial

Table 3
Reactive Fe species and calculated Fe isotope fractions for *Geobacter sulfurreducens* reduction of hematite.

Day	Reduction rate[a] (%Fe(II)/d)	$Fe(II)_{aq}$ (mM)	$Fe(II)_{sorb}$ (mM)	$Fe(III)_{reac}$[b] (mM)	Tot Reac Fe pool[c] (mM)	X–$Fe(II)_{aq}$[d]	X–$Fe(II)_{sorb}$	X $Fe(III)_{reac}$	$\Delta Fe(II)_{aq}$ – $Fe(II)_{sorb}$	2σ error[e]	$\Delta Fe(II)_{aq}$– $Fe(III)_{reac}$	2σ error	$\Delta Fe(II)_{sorb}$– $Fe(III)_{reac}$	2σ error
With Si at pH 7 experiment														
8	3.54E−02	0.145	0.079	0.117	0.341	0.43	0.23	0.34	−0.29	0.08	−2.70	0.36	−2.41	0.37
13	2.45E−02	0.236	0.422	0.619	1.277	0.18	0.33	0.48	−0.31	0.08	−1.57	0.12	−1.27	0.15
20	1.47E−02	0.322	0.325	0.410	1.057	0.30	0.31	0.39	−0.24	0.08	−1.63	0.16	−1.39	0.18
40	3.40E−03	0.486	0.390	0.332	1.209	0.40	0.32	0.27	−0.17	0.08	−1.94	0.30	−1.77	0.31
60	7.85E−04	0.414	0.376	0.310	1.100	0.38	0.34	0.28	0.00	0.08	−1.66	0.19	−1.67	0.21
Without Si a t pH 7 experiment														
8	2.73E−02	0.292	0.165	0.368	0.825	0.35	0.20	0.45	−0.40	0.08	−2.75	0.17	−2.34	0.19
13	1.06E−02	0.322	0.314	0.648	1.284	0.25	0.24	0.50	−0.48	0.08	−2.41	0.11	−1.92	0.14
20	2.80E−03	0.347	0.249	0.497	1.093	0.32	0.23	0.45	−0.44	0.08	−2.66	0.14	−2.22	0.16
40	6.31E−05	0.421	0.375	0.626	1.423	0.30	0.26	0.44	−0.53	0.08	−2.75	0.14	−2.21	0.16
60	1.42E−06	0.415	0.211	0.624	1.250	0.33	0.17	0.50	−0.57	0.08	−2.61	0.16	−2.03	0.18
With Si at pH 8.7 experiment														
8	3.40E−03	0.014	0.041	0.280	0.335	0.04	0.12	0.84	–	–	–	–	−1.16	0.15
13	1.42E−03	0.009	0.054	0.573	0.636	0.01	0.09	0.90	–	–	–	–	−1.22	0.11
20	4.15E−04	0.011	0.058	0.159	0.227	0.05	0.25	0.70	–	–	–	–	−1.74	0.15
40	1.25E−05	0.009	0.084	0.101	0.193	0.05	0.43	0.52	–	–	–	–	−2.57	0.26
60	3.76E−07	0.007	0.066	0.078	0.151	0.05	0.44	0.51	–	–	–	–	−2.74	0.25
Without Si at pH 8.7 experiment														
8	1.73E−02	0.008	0.159	0.157	0.323	0.02	0.49	0.48	–	–	–	–	−1.94	0.14
13	9.11E−03	0.004	0.371	0.517	0.892	0.00	0.42	0.58	–	–	–	–	−1.56	0.11
20	3.72E−03	0.008	0.365	0.365	0.737	0.01	0.49	0.49	–	–	–	–	−1.75	0.12
40	2.88E−04	0.014	0.385	0.332	0.731	0.02	0.53	0.45	–	–	–	–	−1.95	0.15
60	2.23E−05	0.009	0.252	0.202	0.463	0.02	0.54	0.44	–	–	–	–	−1.75	0.14

[a] Rate of reduction, in percentage Fe(II) reduced per day, calculated from the first-order rate law: $[Fe(II)_{Tot}](t) = [Fe(II)_{Tot}]_{max}(1 - e^{-kt})$, where regression of the measured date produced $k = 0.0732$ ($R^2 = 0.916$), 0.1897 ($R^2 = 0.809$), 0.1752 ($R^2 = 0.459$), and 0.1279 ($R^2 = 0.769$) for with Si at pH 7, without Si at pH 7, with Si at pH 8.7, and without Si at pH 8.7 experiments, respectively. Instantaneous reduction rates were determined from the first derivative of the first-order rate law: $d[Fe(II)_{Tot}]/dt = k[Fe(II)_{Tot}]_{max}(e^{-kt})$.

[b] See text for details about calculation of $Fe(III)_{reac}$ concentrations.

[c] Fe_{reac} is the total reactive Fe pool, based on the components that were open to isotopic exchange: $Fe(II)_{aq} + Fe(II)_{sorb} + Fe(III)_{reac}$.

[d] X is the mole fraction of each component out of the total reactive Fe pool.

[e] 2σ errors were generated by the Excel add-in Isoplot, based on uncertainties in isotopic measurements and the fraction of Fe(II) in the 0.5 M HCl extracts.

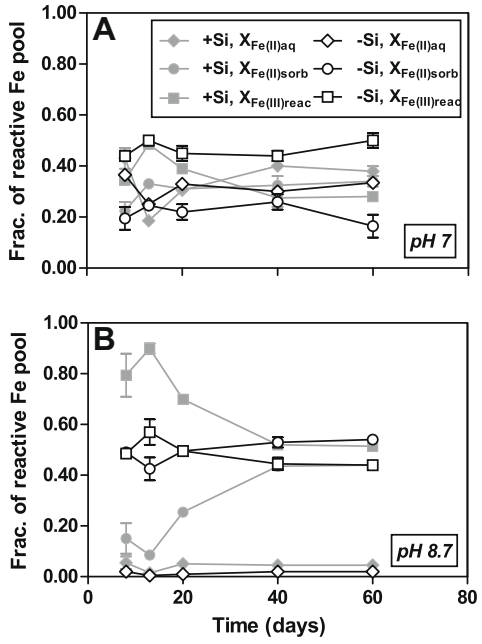

Fig. 8. Temporal variations in the proportions of $Fe(II)_{aq}$, $Fe(II)_{sorb}$, and $Fe(III)_{reac}$ in the reactive Fe pool (see Section 3.5).

reduction. Co-association of Si and Fe with bacterial cell surfaces (Fein et al., 2002) could also have contributed to inhibition of hematite reduction at higher pH, although to our knowledge the nature of cell surface–Si–Fe(II) interactions has not yet been explored. Adsorption of Si onto Fe and Al oxides increases with increasing pH, and reaches a maximum at pH 9 (Hingston and Raupach, 1967; Huang, 1975; Sigg and Stumm, 1981). Adsorption of Si onto Fe oxide surfaces has also been observed in natural environments (Carlson and Schwertmann, 1981; Fortin et al., 1993). It seems likely that the Si in the 0.05 M HCl and 0.5 M HCl extractions included Si adsorbed to the hematite surface, as well as that adsorbed to cell surfaces.

Silica species bound to hematite at high pH may have been in the form of complex Si polymers, given their higher binding affinities with oxide surfaces at high pH relative to monomeric Si species (Stumm et al., 1967; Browman et al., 1989; Meng et al., 2000; Davis et al., 2002). For example, an oligomeric form of Si, containing less than 35 Si atoms, has an affinity for aluminum at least 10^6 times greater than monomeric Si (Taylor et al., 1997). The presence of a polymer layer on the cell surface, coupled with blockage of surface sites by biogenic Fe(II) (as well as perhaps surface Fe(II)–Si phases; see below), are all interpreted to be responsible for suppression of hematite reduction in the presence of Si at pH 8.7.

4.2. Effect of pH and Si on Fe isotope fractionation

Differences in $Fe(II)_{aq}$–$Fe(III)_{reac}$ and $Fe(II)_{sorb}$–$Fe(III)_{reac}$ isotope fractionations as a function of pH and Si (Figs. 6 and 7) may reflect speciation changes among the $Fe(II)_{aq}$, $Fe(II)_{sorb}$, and $Fe(III)_{reac}$ components. It is possible to identify equilibrium isotopic fractionations between these various Fe pools when viewed in terms of changes in the relative molar proportions of the Fe pools. The relatively constant $\Delta^{56}Fe_{Fe(II)aq–Fe(III)reac}$ and $\Delta^{56}Fe_{Fe(II)sorb–Fe(III)reac}$ fractionations over time in the pH 7 no Si experiment (Figs. 6B and 7B, Table 3) suggest steady-state conditions and are inferred to reflect equilibrium fractionations, given the fact that the relative proportions of the reactive Fe components changed little over time (Fig. 8A). The relatively constant $\Delta^{56}Fe_{Fe(II)sorb–Fe(III)reac}$ fractionations (Fig. 7D, Table 3) and reactive Fe pool components (Fig. 8B) over time for the pH 8.7 no Si experiments are similarly inferred to reflect equilibrium fractionations. For reference, the abiologic equilibrium $Fe(II)_{aq}$–hematite fractionation at room temperature is estimated to be $\sim -3.1‰$, as determined by the sum of the equilibrium aqueous Fe(II) ($Fe^{II}(H_2O)_6^{2+}$)–Fe(III) ($Fe^{III}(H_2O)_6^{3+}$) fractionation of $-2.95‰$ (Welch et al., 2003) and the equilibrium aqueous Fe(III)–hematite fractionation of $\sim -0.1‰$ (Skulan et al., 2002). Based on this value, the equilibrium $Fe(II)_{sorb}$–hematite fractionation is estimated to be $-2.6‰$ at room temperature, assuming an average $Fe(II)_{sorb}$–$Fe(II)_{aq}$ fractionation of $+0.5‰$, as determined in this study. The $\Delta^{56}Fe_{Fe(II)sorb–Fe(III)reac}$ equilibrium fractionations in pH 8.7 no Si experiment deviate slightly from those expected for $Fe(II)_{sorb}$–hematite (Fig. 7D), possibly reflecting changes in the speciation of $Fe(II)_{sorb}$ as a function of pH.

It is more difficult to determine if equilibrium isotopic fractionations were attained in the Si added experiments, given their great temporal variation. It is unlikely that the different $Fe(II)_{aq}$–$Fe(III)_{reac}$ and $Fe(II)_{sorb}$–$Fe(III)_{reac}$ fractionations among the experiments reflect significant differences in the speciation of $Fe(II)_{aq}$. The average $\Delta^{56}Fe_{Fe(II)aq–Fe(II)sorb}$ fractionation was $-0.20 \pm 0.16‰$ in pH 7 Si added experiments, which is similar to $-0.49 \pm 0.09‰$ in the pH 7 no Si experiments (Fig. 6). Speciation calculations using Geochemist's Workbench (Bethke, 2002) show that $Fe(II)(OH)^+$ comprises less than 3% of the total aqueous Fe(II) species for all the experiments, suggesting that $Fe(II)_{aq}$ speciation had little impact on the fractionations in our experiments. Formation of an Fe(II)–Si surface species and/or precipitate would also not significantly affect the measured isotopic fractionations because our abiologic experiments showed that the fractionation between aqueous Fe(II) and Fe(II) in Fe–Si gel (Table 4) is essentially identical to the fractionation between $Fe(II)_{aq}$ and $Fe(II)_{sorb}$ in the absence of Si (see Section 3.6). The significantly different $Fe(II)_{aq}$–$Fe(III)_{reac}$ and $Fe(II)_{sorb}$–$Fe(III)_{reac}$ isotope fractionations in Si added experiments may therefore reflect (1) speciation changes in $Fe(II)_{sorb}$ and/or (2) changes in the bonding of Fe in the $Fe(III)_{reac}$ component relative to Fe bonding in hematite.

Adsorption of Si to hematite could have changed the local bonding environment of reactive Fe(III) on the surface by forming Si–O–Fe bonds, thereby altering the $\Delta^{56}Fe_{Fe(II)sorb–Fe(III)reac}$ fractionations (Fig. 1). Silica species have long been recognized as an effective means to stabilize ferrihydrite and inhibit its transformation to more stable minerals such as goethite and hematite (Schwertmann and Taylor, 1989; Schwertmann and Cornell, 1991; Mayer

Table 4
Fe isotope compositions and Fe and Si concentrations of various fractions for abiological control experiments in the presence of silica at pH 8.7.

Experiments	Replicate	Aqueous				Si–Fe gel				Residue in bottles				Filter paper		Total Fe (mM)	System δ^{56}Fe	Total Si (mM)
		Fe(II) (mM)	δ^{56}Fe	Si (mM)	Fe(II) (mM)	δ^{56}Fe	Si (mM)	Fe_{tot} [a] (mM)		δ^{56}Fe	Si (mM)	Fe_{tot} [b] (mM)		δ^{56}Fe	Si (mM)			
Agitated once	1	0.075	−0.98	2.02	0.300	−0.57	0.100	0.089		−0.14	0.090	0.052		−0.15	0.028	0.516	−0.51	2.24
	2	0.068	−0.69	1.95	0.315	−0.65	0.086	0.092		−0.24	0.083	0.068		−0.19	0.016	0.543	−0.53	2.14
Agitated constantly	1	0.078	−1.14	2.11	0.221	−0.58	0.051	0.106		−0.05	0.073	0.096		−0.55	0.013	0.500	−0.55	2.25
	2	0.077	−1.14	2.06	0.206	−0.57	0.095	0.144		−0.16	0.094	0.096		−0.64	0.017	0.524	−0.55	2.27

[a] Twenty percent of the Fe_{tot} was Fe(III), accounting for ~4% of total Fe in the system, possibly due to oxidation during sampling.
[b] Filter paper was dissolved in 7 M HCl so no Fe(II) and Fe(III) was separated for measurement.

and Jarrell, 1996). Schwertmann and Thalmann (1976) and Carlson and Schwertmann (1981) speculated that Si–O–Fe bonds were probably responsible for this stabilization. The nature of Si–O–Fe bonds in oxides have been studied by infrared spectroscopy (e.g., Vempati and Loeppert, 1989), and surface complexation modeling has shown that Si species bind directly to iron oxide/hydroxide surfaces through inner-sphere complexes (Sigg and Stumm, 1981; Barrow and Bowden, 1987), restricting crystal growth by sorption to growth sites (Karim, 1984; Quin et al., 1988; Zhao et al., 1994). Experimental studies using Fe K-edge EXAFS (Extended X-ray Absorption Fine Structure) spectroscopy has shown that Si ligands strongly influence the atomic environments of Fe during hydrolysis of Fe(III), and when Si/Fe>1, Si ligands inhibit corner-sharing Fe octahedral linkages and promote a two-dimensional growth of Fe species through edge-sharing linkages (Doelsch et al., 2000; Mason et al., 2001). More recent work using Fourier transform infrared (FTIR) and Nuclear Magnetic Resonance (NMR) spectroscopy found that with increasing pH, more Si atoms occur in the vicinity of Fe(III) atoms, forming Si–O–Fe bonds that are stable enough and restrict displacement by OH^- ions (Doelsch et al., 2001; Doelsch et al., 2003).

The presence of Si in ferrihydrite affects its transformation to hematite, suggesting that Si influences Fe bonding environments, where Vempati and Loeppert (1989) detected differences in lattice vibration of IR spectra between hematite formed from Si-containing ferrihydrite and that formed in the absence of Si. Campbell et al. (2002) proposed that structural incorporation of Si into hematite formed by heating Si-bearing ferrihydrite caused deformation of the hematite unit cell, producing a net decrease in the number of Fe(III) ions per unit cell. The geometry and structure of the iron silicate complexes formed at the surfaces of iron oxy-hydroxides are expected to be similar to that found for the Fe–Si aqueous solutions, where Si substitutes for double-corner FeO_6 octahedra in iron oxy-hydroxide polymeric complexes (Pokrovski et al., 2003). Because polymerization of Si can occur on the time scale of days to years (Iler, 1979), it is reasonable to speculate that growth of Si polymers with time affected bonding in the reactive Fe(III) component on the time scale of our experiments, thus explaining the temporal variations of the $Fe(II)_{sorb}$–$Fe(III)_{reac}$ fractionations in the Si added experiments (Fig. 6A and C).

Based on the moles of the $Fe(III)_{reac}$ component calculated from isotopic mass balance (Eq. (5)) and average diameter of the hematite substrate (measured by TEM), the $Fe(III)_{reac}$ sampled in the HCl extractions is equivalent to an Fe monolayer in thickness. It therefore seems reasonable that lattice distortions and Si polymerization could have affected Fe in the $Fe(III)_{reac}$ component (Fig. 1). Because stable isotope fractionations reflect fundamental differences in bonding environments (e.g., Schauble, 2004), the changes in $Fe(II)_{sorb}$–$Fe(III)_{reac}$ fractionations in the Si added experiments are interpreted to reflect these changes in Fe bonding relative to the initial hematite substrate. Changes in Fe(III) bonding following Fe(II)–iron oxide/hydroxide interactions has been demonstrated using

^{57}Fe Mössbauer spectroscopy studies of hematite, goethite, and ferrihydrite (Williams and Scherer, 2004; Larese-Casanova and Scherer, 2007). Finally, our assertion that the different Fe(II)–Fe(III)$_{reac}$ fractionations may, in at least some cases, reflect different bonding environments for Fe in the Fe(III)$_{reac}$ component is supported by predicted Fe isotope fractionations among various Fe(III) oxides and hydroxides. Polyakov and Mineev (2000) and Polyakov et al. (2007) predict that at 30 °C, goethite should have a δ^{56}Fe value that is 2.1‰ lower than hematite, and lepidocrocite should have a δ^{56}Fe value that is 2.5‰ lower than hematite, providing some indication of the possible changes in isotopic fractionation among the Fe(III) oxide/hydroxides due to bonding differences. Although such differences have not been confirmed experimentally, and we cannot independently identify the mineralogy of the Fe(III)$_{reac}$ component in our experiments, these observations are consistent with our hypothesis. Our results also demonstrate how stable Fe isotope analysis may be used to explore changes in Fe bonding on the surface of oxide minerals.

4.3. Application to the Precambrian oceans

The largest excursion in δ^{56}Fe values for marine sedimentary rocks occurred in the Neoarchean and continued into the Paleoproterozoic. For example, sedimentary pyrite and C-rich shales between 2.7 and 2.5 Ga has significantly negative δ^{56}Fe values, in contrast to the general near-zero or slightly positive values for Proterozoic-age pyrite and C-rich shales (Rouxel et al., 2005; Yamaguchi et al., 2005; Johnson et al., 2008b). Contrasting proposals have been made to explain this excursion, including extensive oxide precipitation (Rouxel et al., 2005) or cycling by Fe-reducing bacteria (Johnson et al., 2008b). Rouxel et al. (2005) interpreted the isotopic compositions of these sedimentary rocks to directly reflect those of ancient seawater, where light δ^{56}Fe values could be produced by extensive oxide precipitation. However, the inferred large fluctuations in Fe isotope compositions of seawater are considered unlikely when the possible Fe residence times in the Archean oceans are taken into account (Johnson et al., 2008b). Several studies have argued that microbial Fe reduction is the most likely explanation for producing low-δ^{56}Fe, Fe-rich sedimentary rocks because extensive oxide precipitation will produce low-δ^{56}Fe values but very low Fe contents (Johnson et al., 2008a; Severmann et al., 2008). Our experimental results indicate that microbial reduction of hematite is certainly capable of producing low-δ^{56}Fe Fe(II) under conditions of high dissolved Si and over a range of pH conditions. Under conditions of high pH, the majority of Fe(II) produced exists as sorbed Fe(II) on the hematite surface, including Fe–Si polymers in the presence of mM dissolved Si. Our experiments, however, probably represent an end-member case, because it is expected that microbial Fe reduction in natural environments in the Precambrian would likely involve poorly crystalline ferric oxy-hydroxides such as ferrihydrite, which would undergo much more extensive microbial reductive dissolution (e.g., Lovley, 1991; Zachara et al., 1998; Roden, 2003). The smaller Fe(II)–Fe(III)$_{reac}$ fractionations that are produced at elevated pH and in the presence of Si (relative to neutral pH conditions in the absence of Si), indicates that greater extents of microbial Fe cycling would be required to produce a large inventory of low-δ^{56}Fe Fe in the marine sedimentary rock record. Successive reduction–oxidation cycles seem the most likely way very low-δ^{56}Fe values would be produced by bacterial Fe reduction (Johnson and Beard, 2006; Severmann et al., 2006, 2008). It remains unknown, however, if such effects are seen during microbial reduction of ferrihydrite.

The strong effect of pH on the extent and magnitude of isotopic fractionation, particularly in the presence of dissolved Si, highlights the importance of constraining the pH of the Precambrian oceans. Estimates for the pH of the Precambrian oceans vary greatly. Kempe and Degens (1985) suggested that bicarbonate contents in Precambrian seawater significantly exceeded those of Ca, requiring a pH greater than 9. Ohmoto et al. (2004) calculated the pCO_2 required to stabilize siderite, and estimated that Precambrian seawater had a pH range of 5.5–7.5. Grotzinger and Kasting (1993) estimated a more modest drop in pH due to elevated pCO_2 contents in the Precambrian, suggesting that seawater pH may have ranged between 7.5 and 8, only slightly lower than the modern value of 8.1. In addition to the uncertainties in constraining pH of Precambrian seawater, it is possible that the pH of pore fluids in authigenic and early diagenetic environments where microbial Fe reduction may have occurred were different. For example, Klein (2005) calculates that pH must have exceeded 8 to explain the co-occurrence of greenalite, magnetite, and siderite, the earliest Fe–Si–O–CO_3 authigenic and diagenetic phases formed during banded iron formation genesis. Although the pH range of our experiments spans most of these estimates for Precambrian seawater or authigenic/early diagenetic mineral formation, constraining the specific Fe isotope effects that would be expected during microbial Fe reduction will require well-constrained estimates of paleo pH.

5. CONCLUSIONS

New experimental work has expanded our knowledge of the conditions under which microbial Fe(III) oxide reduction produces significant Fe isotope fractionation, including mildly alkaline pH and the presence of dissolved Si, providing a closer analog to conditions that may have existed in ancient marine settings. Our experiments used hematite as the substrate because abiologic Fe(II)–Fe_2O_3 isotopic fractionations have been determined by previous experimental studies, providing an important reference frame for interpreting biological experiments, and hematite is amenable to partial acid dissolution to investigate subcomponents that underwent isotopic exchange. Isotopic fractionations between aqueous and sorbed Fe(II) were essentially constant in all of the hematite reduction experiments, regardless of pH or the presence or absence of Si, and these fractionations were essentially the same as those determined between Fe(II)$_{aq}$ and Fe–Si gels in separate abiologic experiments. In contrast, the isotopic fractionations between Fe(II)$_{aq}$ or Fe(II)$_{sorb}$ and Fe(III)$_{reac}$ often deviated signifi-

cantly from those expected for $Fe(II)_{aq}$–hematite and $Fe(II)_{sorb}$–hematite, based on known equilibrium aqueous $Fe(III)_{aq}$–hematite, $Fe(III)_{aq}$–$Fe(II)_{aq}$, and $Fe(II)_{aq}$–$Fe(II)_{sorb}$ fractionations. Given the constant and similar $Fe(II)_{aq}$–$Fe(II)_{sorb}$ and $Fe(II)_{aq}$–Fe–Si gel fractionations, these differences most likely reflect changes in Fe bonding in the $Fe(III)_{reac}$ component. Deviations from the expected $Fe(II)_{aq}$–hematite and $Fe(II)_{sorb}$–hematite fractionations were most significant for the Si-bearing experiments, and we suggest that this can be attributed to changes in Si–O–Fe bonding of the oxide surface. The 1–2‰ shifts in fractionations involving $Fe(III)_{reac}$ are similar to the shifts predicted to occur between Fe(III) oxide (hematite) and Fe(III) hydroxide (goethite, lepidocrocite) based on theory (Polyakov and Mineev, 2000; Polyakov et al., 2007), providing support for the hypothesis that changes in surface Fe(III) bonding may be reflected in stable isotope fractionations.

Our results demonstrate that microbial Fe reduction is a viable mechanism for producing Fe(II) that has negative δ^{56}Fe values, even under conditions of elevated pH and dissolved Si that may have characterized ancient ocean waters. Results obtained with hematite, which is less reactive than poorly crystalline Fe(III) hydroxides (ferrihydrite) likely represent an end-member case, and we would expect microbial Fe(III) oxide reduction in ancient marine environments to be more extensive than those observed in our experiments if ferrihydrite was the substrate. It is as yet unknown, however, if the same isotopic effects of pH and Si occur in ferrihydrite-reducing systems. The important effect of pH on the extent of Fe isotope fractionation during DIR highlights the importance of inferring the paleo pH of ancient seawater or authigenic/early diagenic marine environments when applying the experimental results obtained here to the ancient rock record.

ACKNOWLEDGMENTS

The authors thank Nita Sahai for insightful discussions about changes in bonding environments for Fe(III) in hematite in the presence of Si. Evgenya S. Shebobolina is thanked for her help with bacterial culturing. Tao Wu is thanked for his help in the preliminary experiments. Constructive criticism by Matthew S. Fantle and an anonymous reviewer and the Associate Editor, James Farquhar, improved the manuscript. This research was supported by the NASA Astrobiology Institute, as well as the National Science Foundation, Research in Biogeosciences Program.

APPENDIX A. SUPPLEMENTARY DATA

Supplementary data associated with this article can be found, in the online version, at doi:10.1016/j.gca.2009.06.026.

REFERENCES

Barrow N. J. and Bowden J. W. (1987) A comparison of models for describing the adsorption of anions A on a variable charge mineral surface. *J. Colloid Interface Sci.* **119**(1), 236–250.

Beard B. L., Johnson C. M., Cox L., Sun H. and Nealson K. H. (1999) Iron isotope biosignatures. *Science* **285**, 1889–1892.

Beard B. L., Johnson C. M., Skulan J. L., Nealson K. H. and Cox L., et al. (2003) Application of Fe isotopes to tracing the geochemical and biological cycling of Fe. *Chem. Geol.* **195**(1–4), 87–117.

Bergquist B. A. and Boyle E. A. (2006) Iron isotopes in the Amazon River system: weathering and transport signatures. *Earth Planet. Sci. Lett.* **248**(1–2), 54–68.

Bethke C. M. (2002) *The Geochemist's Workbench 4.0*.

Browman M. G., Robinson R. B. and Reed G. D. (1989) Silica polymerization and other factors in iron control by sodium silicate and sodium hypochlorite additions. *Environ. Sci. Technol.* **23**(5), 566–572.

Caccavo F., Blakemore R. and Lovely D. (1992) A hydrogen-oxidizing, Fe(III)-reducing microorganism from the Great Bay Estuary, New Hapshire. *Appl. Environ. Microbiol.* **58**, 3211–3216.

Campbell A. S., Schwertmann U., Stanjek H., Friedl J. and Kyek A., et al. (2002) Si incorporation into hematite by heating Si-ferrihydrite. *Langmuir* **18**(21), 7804–7809.

Carlson L. and Schwertmann U. (1981) Natural ferrihydrites in surface deposits from Finland and their association with silica. *Geochim. Cosmochim. Acta* **45**(3), 421–425.

Cloud, Jr., P. E. (1965) Significance of the Gunflint (Precambrian) microflora. *Science* **148**(3666), 27–35.

Crosby H. A., Johnson C. M., Roden E. E. and Beard B. L. (2005) Coupled Fe(II)–Fe(III) electron and atom exchange as a mechanism for Fe isotope fractionation during dissimilatory iron oxide reduction. *Environ. Sci. Technol.* **39**, 6698–6704.

Crosby H. A., Roden E. E., Johnson C. M. and Beard B. L. (2007) The mechanisms of iron isotope fractionation produced during dissimilatory Fe(III) reduction by *Shewanella putrefaciens* and *Geobacter sulfurreducens*. *Geobiology*. doi: 10.1111/j.1472-4669.2007.00103.x.

Davis C. C., Chen H. W. and Edwards M. (2002) Modeling silica sorption to iron hydroxide. *Environ. Sci. Technol.* **36**(4), 582–587.

Doelsch E., Masion A., Rose J., Stone W. E. E. and Bottero J. Y., et al. (2003) Chemistry and structure of colloids obtained by hydrolysis of Fe(III) in the presence of SiO_4 ligands. *Colloids Surf. A* **217**, 121–128.

Doelsch E., Rose J., Masion A., Bottero J. Y. and Nahon D., et al. (2000) Speciation and crystal chemistry of iron(III) chloride hydrolyzed in the presence of SiO_4 ligands. 1. An Fe K-edge EXAFS study. *Langmuir* **16**, 4726–4731.

Doelsch E., Stone W. E. E., Petit S., Masion A. and Rose J., et al. (2001) Speciation and crystal chemistry of Fe(III) chloride hydrolyzed in the presence of SiO_4 ligands. 2. Characterization of Si–Fe aggregates by FTIR and ^{29}Si solid-state NMR. *Langmuir* **17**, 1399–1405.

Fein J. B., Scott S. and Rivera N. (2002) The effect of Fe on Si adsorption by *Bacillus subtilis* cell walls; insights into non-metabolic bacterial precipitation of silicate minerals. *Chem. Geol.* **182**(2–4), 265–273.

Fortin D., Leppard G. G. and Tessier A. (1993) Characteristics of lacustrine diagenetic iron oxyhydroxides. *Geochim. Cosmochim. Acta* **57**(18), 4391–4404.

Garrels R. M., Perry E. A. and Mackenzie F. T. (1973) Genesis of Precambrian iron-formations and the development of atmospheric oxygen. *Econ. Geol.* **68**, 1173–1179.

Grotzinger J. P. and Kasting J. F. (1993) New constraints on Precambrian ocean composition. *J. Geol.* **101**, 235–243.

Hingston F. J. and Raupach M. (1967) The reaction between monosilicic acid and aluminium hydroxide. I. Kinetics of adsorption of silicic acid by aluminium hydroxide. *Aust. J. Soil Res.* **5**(2), 295–309.

Huang C. P. (1975) The removal of aqueous silica from dilute aqueous solution. *Earth Planet. Sci. Lett.* **27**(2), 265–274.

Iler R. K. (1979) *The Chemistry of Silica. Solubility, Polymerisation, Colloid and Surface Properties and Biochemistry*. Wiley.

Jenkyns H., Matthews A., Tsikos H. and Erel Y. (2007) Nitrate reduction, sulfate reduction and sedimentary iron-isotope evolution during the Cenomanian-Turonian Anoxic Event. *Paleoceanography* **22**, PA3208.

Jeon B.-H., Dempsey B. A., Burgos W. D. and Royer R. A. (2001) Reactions of ferrous iron with hematite. *Colloids Surf. A* **191**, 41–55.

Johnson C. and Beard B. (2006) Fe isotopes: an emerging technique in understanding modern and ancient biogeochemical cycles. *GSA Today* **16**, 4–10.

Johnson C. M., Beard B. L., Klein C., Beukes N. J. and Roden E. E. (2008a) Iron isotopes constrain biologic and abiologic processes in banded iron formation genesis. *Geochim. Cosmochim. Acta* **72**(1), 151–169.

Johnson C. M., Beard B. L. and Roden E. E. (2008b) The iron isotope fingerprints of redox and biogeochemical cycling in modern and ancient Earth. *Annu. Rev. Earth Planet. Sci.* **36**, 457–493.

Karim Z. (1984) Characterization of ferrihydrites formed by oxidation of $FeCl_2$ solutions containing different amounts of silica. *Clay Clay Miner.* **32**(3), 181–184.

Kempe S. and Degens E. T. (1985) An early soda ocean? *Chem. Geol.* **53**(1–2), 95–108.

Klein C. (2005) Some Precambrian banded iron-formations (BIFs) from around the world: their age, geologic setting, mineralogy, metamorphism, geochemistry, and origins. *Am. Mineral.* **90**(10), 1473–1499.

Konhauser K. O., Lalonde S. V., Amskold L. and Holland H. D. (2007) Was there really an Archean phosphate crisis? *Science* **315**, 1234.

Larese-Casanova P. and Scherer M. M. (2007) Fe(II) sorption on hematite: new insights based on spectroscopic measurements. *Environ. Sci. Technol.* **41**(2), 471–477.

Liger E., Charlet L. and Van Cappellen P. (1999) Surface catalysis of uranium(VI) reduction by iron(II). *Geochim. Cosmochim. Acta* **63**(19–20), 2939–2955.

Lovley D. (1991) Dissimilatory Fe(III) and Mn(IV) reduction. *Microbiol. Rev.* **55**(2), 259–287.

Lovley D. R. (2000) Fe(III) and Mn(IV) reduction. In *Environmental Metal–Microbe Interactions* (ed. D. R. Lovley). ASM Press, pp. 3–30.

Ludwig K. R. (1991) *ISOPLOT: A Plotting and Regression Program for Radiogenic-Isotope Data, Version 2.53*. US Geological Survey.

Maliva R. G., Knoll A. H. and Simonson B. M. (2005) Secular change in the Precambrian silica cycle: insights from chert petrology. *Geol. Soc. Am. Bull.* **117**(7), 835–845.

Masion A., Doelsch E., Rose J., Moustier S. and Bottero J. Y., et al. (2001) Speciation and crystal chemistry of iron(III) chloride hydrolyzed in the presence of SiO_4 ligands. 3. Semilocal scale structure of the aggregates. *Langmuir* **17**, 4753–4757.

Mayer T. D. and Jarrell W. M. (1996) Formation and stability of iron(II) oxidation products under natural concentrations of dissolved silica. *Water Res.* **30**(5), 1208–1214.

Meng X., Bang S. and Korfiatis G. P. (2000) Effects of silicate, sulfate, and carbonate on arsenic removal by ferric chloride. *Water Res.* **34**(4), 1255–1261.

Ohmoto H., Watanabe Y. and Kumazawa K. (2004) Evidence from massive siderite beds for a CO_2-rich atmosphere before 1.8 billion years ago. *Nature* **429**, 395–399.

Pokrovski G. S., Schott J., Farges F. and Hazemann J.-L. (2003) Iron (III)–silica interactions in aqueous solution: insights from X-ray absorption fine structure spectroscopy. *Geochim. Cosmochim. Acta* **67**(19), 3559–3573.

Polyakov V. B., Clayton R. N., Horita J. and Mineev S. D. (2007) Equilibrium iron isotope fractionation factors of minerals: reevaluation from the data of nuclear inelastic resonant X-ray scattering and Mössbauer spectroscopy. *Geochim. Cosmochim. Acta* **71**(15), 3833–3846.

Polyakov V. B. and Mineev S. D. (2000) The use of Mössbauer spectroscopy in stable isotope geochemistry. *Geochim. Cosmochim. Acta* **64**(5), 849–865.

Quin T. G., Long G. J., Benson C. G., Mann S. and Williams R. J. P. (1988) Influence of silicon and phosphorus on structural and magnetic properties of synthetic goethite and related oxides. *Clay Clay Miner.* **36**(2), 165–175.

Roden E. E. (2003) Fe(III) oxide reactivity toward biological versus chemical reduction. *Environ. Sci. Technol.* **37**, 1319–1324.

Roden E. E. (2004) Analysis of long-term bacterial vs. chemical Fe(III) oxide reduction kinetics. *Geochim. Cosmochim. Acta* **68**(15), 3205–3216.

Roden E. E. (2008) Microbiological controls on geochemical kinetics 1: fundamentals and case study on microbial Fe(III) reduction. In *Kinetics of Water–Rock Interactions* (eds. S. L. Brantley, J. D. Kubicki and A. F. White). Springer, pp. 335–415.

Roden E. E. and Urrutia M. M. (1999) Ferrous iron removal promotes microbial reduction of crystalline iron(III) oxides. *Environ. Sci. Technol.* **33**, 1847–1853.

Roden E. E. and Urrutia M. M. (2002) Influence of biogenic Fe(II) on bacterial crystalline Fe(III) oxide reduction. *Geomicrobiol. J.* **19**, 209–251.

Rouxel O. J., Bekker A. and Edwards K. J. (2005) Iron isotope constraints on the Archean and Paleoproterozoic ocean redox state. *Science* **307**, 1088–1091.

Schauble E. A. (2004) Applying stable isotope fractionation theory to new systems. *Rev. Mineral. Geochem.* **55**(1), 65–111.

Schwertmann U. and Cornell R. M. (1991) *Iron Oxides in the Laboratory: Preparation and Characterization*. VCH.

Schwertmann U. and Taylor R. M. (1989) Iron oxides. In *Minerals in Soil Environments* (eds. J. B. Dixon and S. B. Weed). Soil Science Society of America.

Schwertmann U. and Thalmann H. (1976) The influence of [Fe(II)], [Si], and pH on the formation of lepidocrocite and ferrihydrite during oxidation of aqueous $FeCl_2$ solutions. *Clay Miner.* **11**, 189–200.

Severmann S., Johnson C. M., Beard B. L. and McManus J. (2006) The effect of early diagenesis on the Fe isotope compositions of porewaters and authigenic minerals in continental margin sediments. *Geochim. Cosmochim. Acta* **70**(8), 2006–2022.

Severmann S., Lyons T. W., Anbar A., McManus J. and Gordon G. (2008) Modern iron isotope perspective on the benthic iron shuttle and the redox evolution of ancient oceans. *Geology* **36**(6), 487–490.

Sigg L. and Stumm W. (1981) The interaction of anions and weak acids with the hydrous goethite (α-FeOOH) surface. *Colloids Surf.* **2**(2), 101–117.

Skulan J. L., Beard B. L. and Johnson C. M. (2002) Kinetic and equilibrium Fe isotope fractionation between aqueous Fe(III) and hematite. *Geochim. Cosmochim. Acta* **66**(17), 2995–3015.

Staubwasser M., von Blanckenburg F. and Schoenberg R. (2004) Iron isotopes in the early marine diagenetic iron cycle. *Geology* **34**(8), 629–632.

Stookey L. (1970) Ferrozine: a new spectrophotometric reagent for iron. *Anal. Chem.* **42**, 779–781.

Strathmann T. J. and Stone A. T. (2003) Mineral surface catalysis of reactions between FeII and oxime carbamate pesticides. *Geochim. Cosmochim. Acta* **67**(15), 2775–2791.

Stumm W. (1992) *Chemistry of the Solid–Water Interface*. John Wiley & Sons, Inc.

Stumm W., Huper H. and Champlin R. L. (1967) Formulation of polysilicates as determined by coagulation effects. *Environ. Sci. Technol.* **1**(3), 221–227.

Taylor P. D., Jugdaohsingh R. and Powell J. J. (1997) Soluble silica with high affinity for aluminum under physiological and natural conditions. *J. Am. Chem. Soc.* **119**(38), 8852–8856.

Thamdrup B. (2000) Bacterial manganese and iron reduction in aquatic sediments. *Adv. Microb. Ecol.* **16**, 41–84.

Urrutia M. M., Roden E. E., Fredrickson J. K. Z. and Zachara J. M. (1998) Microbial and geochemical controls on synthetic Fe(III) oxide reduction by *Shewanella alga* strain BrY. *Geomicrobiol. J.* **15**, 269–291.

Vempati R. K. and Loeppert R. H. (1989) Influence of structural and adsorbed Si on the transformation of synthetic ferrihydrite. *Clay Clay Miner.* **37**, 273–279.

Welch S. A., Beard B. L., Johnson C. M. and Braterman P. S. (2003) Kinetic and equilibrium Fe isotope fractionation between aqueous Fe(II) and Fe(III). *Geochim. Cosmochim. Acta* **67**(22), 4231–4250.

Widdel F., Schnell S., Heising S., Ehrenreich A. and Assmus B., et al. (1993) Ferrous iron oxidation by anoxygenic phototrophic bacteria. *Nature* **362**, 834–836.

Williams A. G. B. and Scherer M. M. (2004) Spectroscopic evidence for Fe(II)–Fe(III) electron transfer at the Fe oxide–water interface. *Environ. Sci. Technol.* **38**(18), 4782–4790.

Yamaguchi K. E., Johnson C. M., Beard B. L. and Ohmoto H. (2005) Biogeochemical cycling of iron in the Archean–Paleoproterozoic Earth: constraints from iron isotope variations in sedimentary rocks from the Kaapvaal and Pilbara Cratons. *Chem. Geol.* **218**(1–2), 135–169.

Zachara J. M., Fredrickson J. K., Li S.-M., Kennedy D. W. and Smith S. C., et al. (1998) Bacterial reduction of crystalline Fe^{3+} oxides in single phase suspensions and subsurface materials. *Am. Mineral.* **83**, 1426–1443.

Zhao J. M., Huggins F. E., Feng Z. and Huffman G. P. (1994) Ferrihydrite – surface-structure and its effects on phase-transformation. *Clay Clay Miner.* **42**(6), 737–746.

Associate editor: James Farquhar